View metadata, citation and similar papers at core.ac.uk

brought to you by CORE

provided by Florence Research

Journal of Power Sources 299 (2015) 391–397

Contents lists available at ScienceDirect

Journal of Power Sources

journal homepage: www.elsevier.com/locate/jpowsour

High volume hydrogen production from the hydrolysis of sodium borohydride using a cobalt catalyst supported on a honeycomb matrix

Andrea Marchionni [a, *], Manuela Bevilacqua [a], Jonathan Filippi [a], Maria G. Folliero [a, b], Massimo Innocenti [a, c], Alessandro Lavacchi [a], Hamish A. Miller [a], Maria V. Pagliaro [a, c], Francesco Vizza [a, **]

[a] Consiglio Nazionale delle Ricerche – Istituto di Chimica dei Composti Organometallici (CNR-ICCOM), Via Madonna del Piano 10, Sesto Fiorentino, 50019, Italy
[b] Università di Siena, Dipartimento di Biotecnologie, Chimica e Farmacia, Via Aldo Moro 2, Siena, 53100, Italy
[c] Università di Firenze, Dipartimento di Chimica, Via della Lastruccia 3, Sesto Fiorentino, 50019, Italy

HIGHLIGHTS

- A Co_xB catalyst supported on Cordierite Honeycomb was synthesized.
- Apparatus for the H_2 generation from the Sodium Borohydride hydrolysis was showed.
- The catalyst was able to evolved up to 35 L min^{-1} g_{Co}^{-1} at 5 bar pressure.
- The apparatus was able to feed a 2 kW scale PEMFC stack in principle.

ARTICLE INFO

Article history:
Received 23 June 2015
Received in revised form
31 August 2015
Accepted 1 September 2015
Available online 15 September 2015

Keywords:
Sodium borohydride hydrolysis
Hydrogen generation
Cobalt
Cordierite monolith
Reactor design

ABSTRACT

Hydrogen storage and distribution will be two very important aspects of any renewable energy infrastructure that uses hydrogen as energy vector. The chemical storage of hydrogen in compounds like sodium borohydride ($NaBH_4$) could play an important role in overcoming current difficulties associated with these aspects. Sodium borohydride is a very attractive material due to its high hydrogen content. In this paper, we describe a reactor where a stable cobalt based catalyst supported on a commercial Cordierite Honeycomb Monolith (CHM) is employed for the hydrolysis of alkaline stabilized $NaBH_4$ (SBH) aqueous solutions. The apparatus is able to operate at up to 5 bar and 130 °C, providing a hydrogen generation rate of up to 32 L min^{-1}.

© 2015 Elsevier B.V. All rights reserved.

1. Introduction

The storage and distribution of hydrogen is one of the most important aspects of a hydrogen based economy [1,2]. The volume required to store 4 kg of hydrogen gas in compressed cylinders at 200 bar is about 225 L. The production and storage of liquefied H_2 is costly, as it requires high-energy input and sophisticated equipment. Alternatively, the use of sodium borohydride ($NaBH_4$, SBH) as a potential hydrogen storage material has attracted significant interest from the late 1990s by virtue of its high Gravimetric Hydrogen Storage Capacity (GHSC) [1,3]. Hydrogen gas can be released from SBH by hydrolysis in the presence of water forming sodium metaborate ($NaBO_2$) and heat (Eq. (1))

$$NaBH_4 + (2+x)H_2O \rightarrow NaBO_2 \cdot x\,H_2O + 4H_2 + \sim 300\ \text{kJ/mol} \quad (1)$$

The value of GHSC depends upon the hydration state of the $NaBO_2$ by-product (GHSC = 10.8% with $x = 0$; GHSC = 7.3% with $x = 2$ and GHSC = 5.5% with $x = 4$). The most common hydration state of sodium metaborate is two [4]. For practical application of the $NaBH_4$–H_2O system for hydrogen generation in a controlled

* Corresponding author.
** Corresponding author.
E-mail addresses: andrea.marchionni@iccom.cnr.it (A. Marchionni), francesco.vizza@iccom.cnr.it (F. Vizza).

http://dx.doi.org/10.1016/j.jpowsour.2015.09.006
0378-7753/© 2015 Elsevier B.V. All rights reserved.

manner, one has to take into account also the stability of $NaBH_4$ solutions given the thermodynamic spontaneity of reaction (1). For this reason alkali metal hydroxides, generally sodium or potassium hydroxides (NaOH or KOH) are used to stabilize $NaBH_4$ in aqueous solutions.

Reaction (1) is a spontaneous and exothermic process that can be accelerated by means of suitable catalysts, generally based on finely dispersed transition metals deposited on metal oxides or carbon supports. Catalysts employed include noble metal salts (Pt, Rh, Ir, Ru) [1,5,6], non-noble metal salts (Mn, Fe, Co, Ni, Cu) [7–9], and metal borides such as cobalt-boride (CoB), cobalt–cobalt boride (Co–CoB) and nickel–cobalt boride (Ni–CoB) which combine excellent catalytic activity with low cost [4,10–14]. The main drawback of the use of such cobalt based catalysts consists in the dramatic loss of activity after only a few operative cycles [10,12,13]. This decrease in activity is believed to be due to the formation of a hydrated salt of sodium metaborate which precipitates and blocks catalytic sites. The solubility of sodium metaborate (28 g in 100 g of H_2O at 25 °C) is lower than that of $NaBH_4$ (55 g in 100 g of H_2O). In order to avoid this deactivation process an initial $NaBH_4$ concentration lower than 16 g in 100 g of water is generally used [10,15]. A number of studies have been published dealing with both the catalytic activity and long-term stability of Co_2–B catalysts doped with either Cr or W [1,4,5,7,13,16,17]. Cobalt oxides have also been extensively studied [14,18,19], using various catalyst supports, like nickel foam [20–22], carbon [23–25], polymers [26–34], soils [35] and minerals [36–38].

Several types of reactors, both static and dynamic have been designed to exploit the SBH reaction. In static devices, the catalyst either a powder, in pellet form or supported on an inert porous material such as honeycomb monoliths, is introduced into a vessel containing the $NaBH_4$ solution [6,39–43]. Static systems exhibit generally low efficiency due to various phenomena including: (a) the difficulty of catalyst separation from the exhaust solution; (b) catalyst leaching from the support, (c) the de-activation of the catalyst due to the precipitation of sodium metaborate and (d) mass transport problems. Dynamic systems are based on the flow of a $NaBH_4$–NaOH solution inside a tubular reactor containing an appropriate catalyst [44]. In a recent example Amendola et al., describe the use of a peristaltic pump that forces the $NaBH_4$ solution to pass through a reactor containing a Ru-based catalyst supported on ion-exchange resins. The reactor is part of the Millennium Cell and Horizon Fuel Cell technology applied to Hydropak generators with a nominal maximum power output of 50 W [45–49]. Kim et al. have reported a system using a Co-based catalyst supported on nickel foam, which feeds H_2 to a 400 W PEM Fuel Cell (Proton Exchange Membrane Fuel Cell) [40]. In another example Arzac et al. used a similar Co catalyst to develop a device which produces and feeds H_2 into a 60 W fuel cell stack [42]. Kojima et al. developed a 10 kW system using 240 g of a Pt–$LiCoO_2$ catalyst confined in a honeycomb monolith. This system was able to produce H_2 with a maximum flow of 120 L min^{-1} at about 110 °C [41].

The state of the art in this field is rather varied with a number of different devices and catalysts described in the literature. It is, however, equally apparent that such devices do not fully satisfy market requirements, regarding various factors that include: (a) low H_2 production capacity, (b) low catalyst stability, (c) the need for frequent catalyst replacement, (d) high catalyst cost, (e) the inability to interrupt hydrogen evolution on demand and (f) the need to use concentrated $NaBH_4$ solutions (more than 15 wt%). Here we describe the design and construction of a SBH reactor that utilizes a cobalt boride (Co_xB) catalyst supported on a commercial Cordierite Honeycomb Monolith (CHM). At ambient pressure, the system produces 7.5 L min^{-1} g_{Co}^{-1} of hydrogen at 70 °C. At 134 °C and 5 bar outlet pressure hydrogen production of up to 32 L min^{-1} g_{Co}^{-1} was obtained. The stability of the catalyst system studied under working conditions showed no significant decrease over up to 10 repeat cycles.

2. Experimental

2.1. General

The Cordierite Honeycomb Monolith (CHM) was purchased from Corning (Celcor® 600/4) and was used as is. All chemicals were purchased from Sigma Aldrich (ACS reagent grade purity) and used without any further purification.

2.2. Synthesis of Co_xB/CHM

The CHM was first cut to size with a base of 20 mm × 22 mm (about 400 cells) and 89 mm tall. The Co_xB/CHM catalyst was prepared as follows. (1) The CHM was dipped in a 0.5 M $Co(CH_3COO)_2 \cdot 4H_2O$ aqueous solution for 30 min, to absorb the cobalt salt precursor, and then drained; 2) dried at 120 °C for 30 min and heated at 400 °C for 40 min to decompose all the acetate to cobalt oxide, as reported by Grimes and Fitch [50]; and 3) cooled in air and weighed to calculate the metal loading of Co_3O_4/CHM. Each deposition cycle only deposits a small amount of metal oxide so it was repeated until the desired metal loading was reached (1.174 g or Co, 8.27 wt.%). The metal content was confirmed with ICP-OES analysis of a small portion of the catalyst. During preparation the colour of the CHM changed from light yellow to dark brown, the colour of cobalt oxide (see Supporting information, Fig. S1). Finally, the Co_3O_4/CHM was dipped in a 13 wt.% SBH aqueous solution for 20 min at room temperature to obtain the active catalyst. The colour of the CHM became immediately black.

2.3. Physical characterization

The samples were characterized by X-ray Powder Diffraction (XRPD), using a PAN analytical X'PERT PRO diffractometer, and by Scanning Electron Microscopy (SEM), acquired by a FEI ESEM Quanta 200 instrument. The XRPD measurements were conducted on a milled fraction of each sample employing CuKα radiation (λ = 1.54187 Å) and a parabolic MPD-mirror. The traces were acquired at room temperature in the 2θ range from 5.0 to 80.0°, using a continuous scan mode with an acquisition step size of 0.0263° and a counting time of 49.5 s. The SEM analysis was conducted on a single wall of the lamellar structure cut from the body of the catalyst.

2.4. Catalytic activity

The catalytic activity was evaluated using a stainless steel reactor, shown schematically in Fig. 1. The reactor was made of a cylindrical stainless steel chamber (diameter 77 mm and height about 40 cm) closed at the bottom with a disk, equipped with a tap to enable removal of the solution from the reactor. On the top, there is a removable head piece, with a stainless steel rod whose vertical movement is controlled by a stepper motor. At the tip of the rod, there is a perforated plastic cylinder as catalyst holder. The head system allows the control of hydrogen evolution thanks to control of the immersion of catalyst in the SBH solution. In the present study, the catalyst was completely immersed into the solution during all experiments. During the experiments conducted at atmosphere pressure, the generated hydrogen passed through a special channel in the head piece connected to a vapour trap and a flow meter, while an adjustable check valve was inserted between

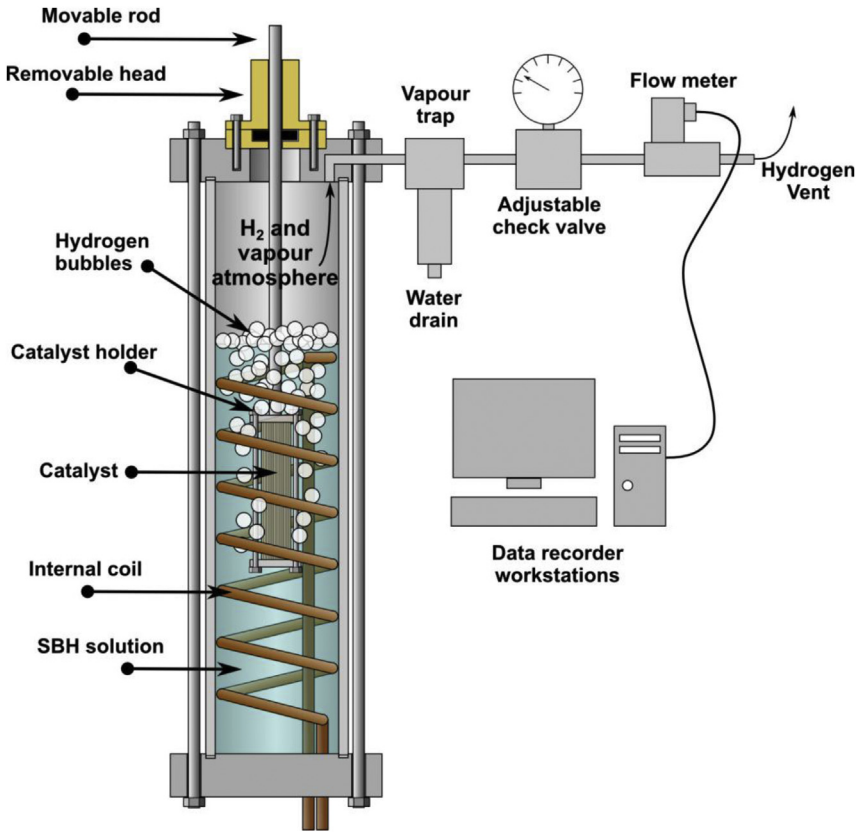

Fig. 1. A schematic representation of the interior of the reactor and the connection with the other parts of the system. A photograph of the real system can be found in the Supporting Information (Fig. S3).

the trap and the flow meter instrument during the high pressure experiments. Inside the reactor, a copper coil was used to control the initial temperature of the solution with circulating warm water (50 °C). The seal of the reactor was tested prior to any experiments using H_2 up to a pressure of 10 bar.

A 3.44 M (ca. 13 wt.%) $NaBH_4$ solution stabilized with 0.5 M (c.a. 2 wt.%) of NaOH was used in all experiments. The actual volume of the solution was about 1.2 L. The hydrogen generation flow was recorded by a Bronkhorst® EL-FLOW® mass flow meter model F-101E-AGD-22-V with maximum flow rate of 10 NL min^{-1} and with a Bronkhorst® EL-FLOW® mass flow meter model F-101E-AGD-22-V with a 200 NL min^{-1} scale to comparison. The generated gas was dried with a two step filter (molecular sieves and a liquid nitrogen trap) before the flow meter. The temperature of the solution was measured with a PIXSYS 171-23ABC-T module connected to a PC. Each experiment was stopped when hydrogen flow ceased. Between two subsequent experiments, the catalyst was washed with deionised water and dried in air.

3. Results and discussion

3.1. Physical characterization

The XRPD patterns of the CHM support, catalyst precursor Co_3O_4/CHM after calcination at 400 °C and catalytic phase are shown in Fig. 2. The CHM support shows typical Bragg reflections of Cordierite with chemical formula $Mg_{1.91}Fe_{0.09}Al_4Si_5O_{18}$ [50], at 10.40°, 18.00°, 18.95°, 21.61°, 26.37°, 28.35°, 29.42°, 33.88°, 38.74° and 54.36° (trace a).

The catalyst precursor also shows the spinel Co_3O_4 (Fd-3m) signals at 31.26° (022), 36.84° (113), 44.80° (004), 59.35° (115) and 65.22° (044) (trace b) [51,52]. Debye–Scherrer analysis [53] indicates an average Co_3O_4 crystallite size of 18.5 nm.

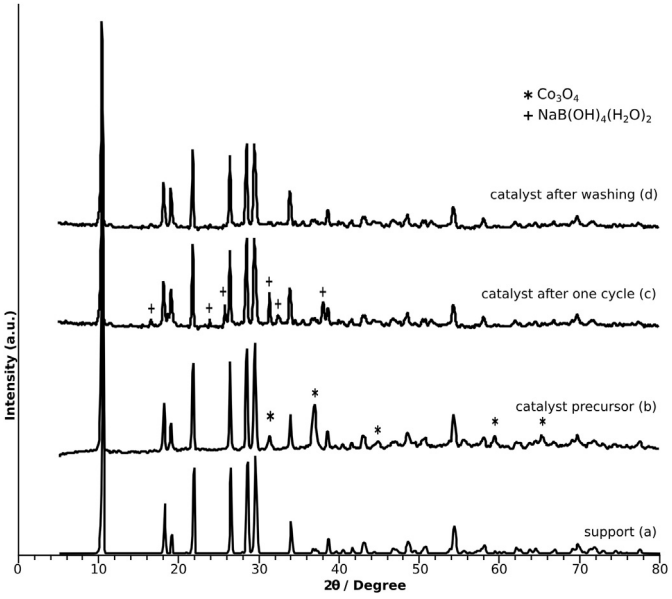

Fig. 2. XRPD patterns of a) CHM support, b) catalyst precursor Co_3O_4/CHM, c) catalyst precursor treated with SBH solution and d) catalyst after rinsing with deionized water. The symbols * and + point out the principal Bragg reflections of Co_3O_4 and sodium metaborate hydrate, respectively.

After treatment with SBH (trace c) signals for $NaB(OH)_4(H_2O)_2$, a

sodium metaborate hydrate phase, are visible at 16.51°, 18.64°, 23.83°, 25.74°, 31.32°, 32.38° and 38.00° [54]. No presence of Co_xB [55,56] or any other Co species was detected even after washing sample c with water (trace d). To understand the reasons for this behaviour, we synthesized Co_xB in powder form not supported on cordierite (see Supporting Information). The XRPD pattern of this material did not show any clearly identified peak for any Co species, suggesting that the Co_xB was in an amorphous phase not detectable by XRPD. For comparison, we analysed also the same Co_xB powder after a heating treatment at 300 °C (to favour sintering) and a commercial (Sigma Aldrich) cobalt boride. Both materials showed peaks (see Fig. S4) with low intensity (large signal to noise ratio). These results support evidence of the presence of an amorphous phase of cobalt boride on the cordierite support.

Scanning electron microscope (SEM) images of the CHM support (Fig. 3A) show the macro channels of the honeycomb structure at low magnification and pores, cavities and surface roughness at high magnification (insert). Energy-dispersive X-ray spectroscopy (EDX) analysis (Fig. S2A–C) confirm the main components of CHM: Mg, Al, and Si. An image of the Co_3O_4/CHM pre-catalyst (Fig. 3B) shows particle aggregates on the surface support ranging from a few μm to 50 μm. The EDX analysis conducted on these particles confirms the presence of Co and O of Co_3O_4, in addition to those of CHM (Fig. S2D–F). The morphology of the catalyst obtained from Co_3O_4/CHM by treatment with SBH (Fig. 3C), changes significantly with respect to Co_3O_4/CHM. In fact, it becomes difficult to see the macro channels of the honeycomb structure of CHM support. Large (100–200 μm) and amorphous particles cover completely the surface. At higher magnification, a layer composed by needles is visible. EDX analysis identified it as sodium borate, in agreement with the pattern *c* of XRD graph (Fig. S2G–I).

After a washing treatment with deionized water, the sodium metaborate in the form of needles disappears from the surface, leaving an amorphous layer. The EDX analysis (Fig. S2J–L) showed a drastic decrease of the metaborate salt (sodium signal), while the signal of boron remains as well as both the signals of Co and support (Mg, Al, Si). This evidence supports the hypothesis of the existence of an amorphous phase of Co_xB, anchored on the support, still covered by some residue of sodium metaborate which has not been completely eliminated by washing with water [52].

To complete the understanding of this morphology behaviour, was also analysed a sample after ten catalytic cycles and the images are reported in Fig. S2M–O. The surface appears very similar to the sample after the first catalytic cycle, meaning that no significant change in morphology occurs over repeated cycling.

3.2. Hydrogen generation

The hydrolysis of $NaBH_4$ was carried out in the stainless steel reactor shown in Fig. 1, the structure of which is described in detail in the experimental section. The main features of the reactor consist of: i) a removable head that allows a vertical movement of a stainless steel rod, on whose tip is installed the catalyst holder, controlled by a stepper motor; and ii) a copper coil with circulating warm water to control the initial temperature of the solution.

The hydrogen generation rate (HGR) can be varied by controlling the immersion of the catalyst in the SBH aqueous solution. In the experiments described here, the catalyst was completely immersed. The solution (1.2 L of a 3.44 M $NaBH_4$ aqueous solution stabilized with NaOH 0.5 M) contained in the reactor was gently

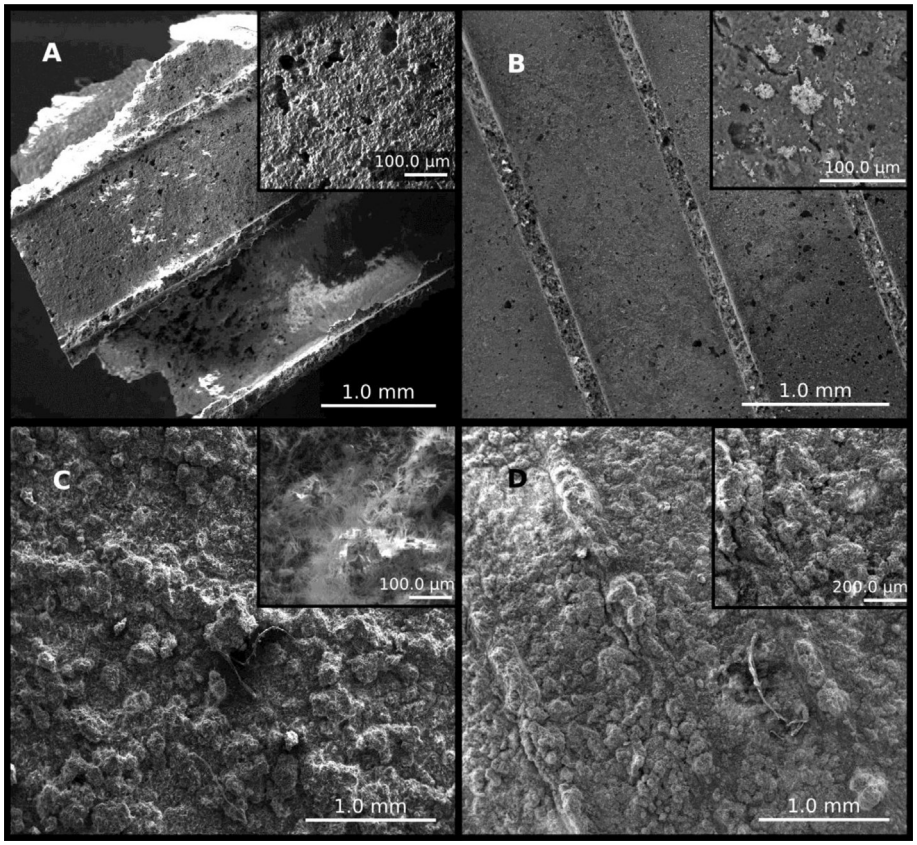

Fig. 3. Representative SEM images at 80× magnification of: a) CHM support, b) Co_3O_4/CHM material, c) Co_xB/CHM catalyst after one cycle and d) used Co_xB/CHM after washing with deionized water. As inserts, related pictures at higher magnifications.

warmed by means of the internal coil to promote the initial stage of the catalytic process [12,15,26].

The pre-catalyst in the form Co_3O_4/CHM, was used in the first cycle of SBH hydrolysis. In this way the catalyst Co_xB was generated *in situ*. In Fig. 4 are reported the profiles performed at ambient pressure of the HGR (lines), reported as L min^{-1} g_{Co}^{-1}, showing the total outflow of hydrogen produced during the first, second and tenth cycle (for comparison, Fig. S6 in the Supporting Information reports the total volume of evolved hydrogen). In all cycles, the HGR showed a bell-like profile. In agreement with the literature data [4,12], the first phase (induction period) where almost no hydrogen evolution is observed lasts approx. 12 min and is due to the formation of active a Co_xB phase from the Co_3O_4; the second phase shows a fast growth of HGR, due to the catalytic activity of the Co_xB phase, which reaches a maximum and, finally, during a third period a decrease of HGR is observed due to the depletion of the SBH in the solution. It has also been proposed that in this third phase, the alkaline pH due to the formation of sodium borate, can also lead to the oxidization of the catalyst Co_xB to hydrated cobalt hydroxide species [10,18,56,57]. This would justify why the induction period remains in the following cycles.

After each cycle, the reactor was emptied and refilled with a fresh solution of SBH. No leaching of cobalt or solid material from the support into the exhaust solution was observed and this was confirmed by ICP-OES analysis of solutions.

The maximum HGR value of 7.2 L min^{-1} g_{Co}^{-1} was reached during the first cycle (Fig. 4), while the second cycle showed a max value of 5.45 L min^{-1} g_{Co}^{-1}, with a decrease of hydrogen evolution of 25%. In the following ten cycles the activity was stable, with a max HGR of about 5.5 L min^{-1} g_{Co}^{-1}. This behaviour is in line with the literature data, in particular as observed by Demirci, Miele and co-workers that explained the decrease in HGR is due to hydrated sodium metaborate ($NaBO_2 \cdot xH_2O$) precipitation on the catalyst surface [58]. Also SEM analysis results reported in Fig. S2M–O show a very similar surface morphology between the samples after the first and the tenth cycle.

The efficiency of hydrogen generation with respect to the theoretical total volume was between 95 and 98% for all cycles. The temperature within the reactor during the first cycle, reached a maximum of ca. 70 °C during the period of maximum hydrogen production (Fig. 4, squares) cooling to 50 °C at the end of the reaction. The increase in temperature is due to the high reaction rate that releases about 3.3 kJ of heat per L of hydrogen produced. A similar trend was observed in the other reaction cycles.

To better understand the role of the CHM support in the catalytic reaction, we studied also the behaviour of a homemade Co_xB powder catalyst (for more details see the Supporting Information). The performance was very good with a maximum HGR of 7.4 L min^{-1} g_{Co}^{-1}, and conversion efficiency of 97% which is very close to the values obtained for the Co_xB/CHM catalyst (see Fig. S5). So we can conclude that the CHM support does not participate in the catalytic reaction, its role being to increase mechanical resistance and adhesion of the catalyst layer. Indeed, when the catalyst was soaked in the SBH solution the evolved hydrogen passed through the internal channels without breaking any of the superficial layers (see Fig. 5). The absence of active phase leaching permits the design and development of real practical devices for the hydrogen generation from SBH hydrolysis. Moreover, the CHM support has a large surface area (34.5 cm^2 cm^{-3}) allowing large dispersion of Co_xB particles.

We also carried out a set of hydrogen evolution experiments at 5 bar outlet pressure, by inserting a check valve in the line between the vapour trap and the flow meter instrument (Fig. 1 and S3) that allows the passage of hydrogen at pressures above 5 bar. In Fig. 6 are reported the HGR and the temperature profiles of the first, second and tenth cycle conducted 5 bar. Also in this case, the HGR showed a bell-like shape but with a narrower profile with respect to the experiments conducted at ambient pressure. The first cycle reached a maximum production of 32.5 L min^{-1} g_{Co}^{-1} while the temperature increased to 134 °C with an efficiency of hydrogen generation of 94%. The second cycle showed a decrease of ca. 25% of the hydrogen flow, while subsequent cycles showed no significant changes in hydrogen productivity. In the exhaust solutions after each test, no residues attributable to leaching of the catalyst were observed.

Here we have exploited the high activity of Co_xB for the hydrolysis of SBH by incorporating the active phase of the catalyst in a high surface area monolith, which combines a high catalyst surface area with improved stability due to strong catalyst–support interactions. During the first cycle of batch experiments, a drop in hydrogen production rate is observed, associated with a complex modification of the catalytic system where cobalt oxides are transformed into Co_xB with co-precipitation of sodium metaborate, while the performance remains stable during further cycles. Theoretically, the generated hydrogen at the ambient pressure experiments would be able to feed a 500 W PEMFC (Proton

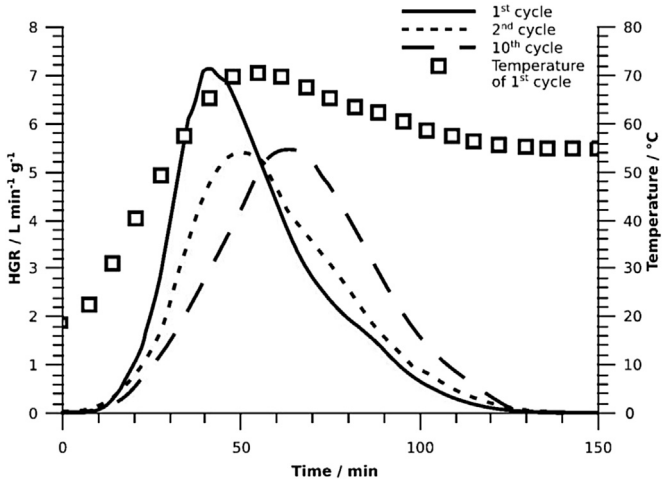

Fig. 4. HGR profiles of the first, second and tenth cycle. The temperature profile (squares) of the first cycle is also shown.

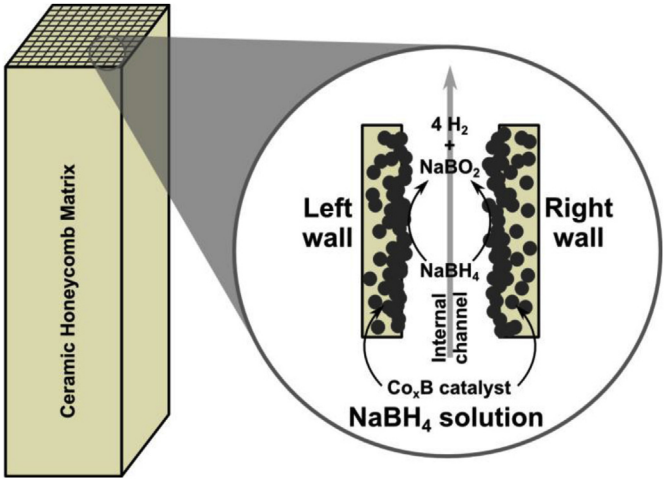

Fig. 5. Proposed diagram of operation of the Co_xB/CHM catalyst. The catalyst surface in each channel on contact with SBH produce hydrogen gas and sodium borate.

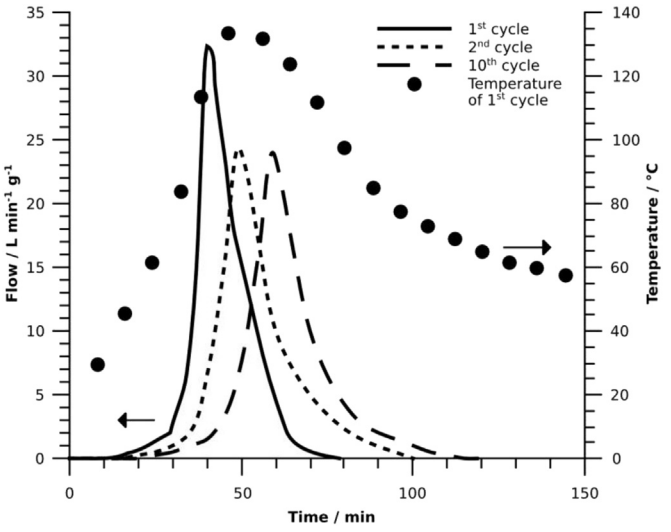

Fig. 6. HGR profiles of the first, second and tenth cycle conducted at 5 bar. The temperature profile (squares) of the first cycle is also shown.

Exchange Membrane Fuel Cell), while the HGR observed during the pressurized experiments at 5 bar would be able to feed a 2 kW size PEMFC stack.

4. Conclusions

In summary, we describe a reactor within which a cobalt-based catalyst supported on a commercial Cordierite Honeycomb Monolith (CHM), is used for the hydrolysis of alkaline stabilized Sodium Borohydride (SBH) aqueous solutions. The apparatus was able to operate at high temperature (>130 °C) and high pressure (5 bar).

The maximum HGR was 7.2 L min^{-1} g_{Co}^{-1} at ambient pressure and 32.5 L min^{-1} g_{Co}^{-1} at 5 bar. The combination of this reactor with a suitable PEMFC stack to form a standalone power unit will form the basis of our future development of this technology.

Acknowledgements

The authors are grateful to Ente Cassa di Risparmio di Firenze for HYDROLAB2 project and to MIUR for FIRB 2010 project RBFR10J4H7_002 for financial support. Many thanks also to Carlo Bartoli for the realization of the reactor.

Appendix A. Supplementary data

Supplementary data related to this article can be found at http://dx.doi.org/10.1016/j.jpowsour.2015.09.006.

References

[1] D.M.F. Santos, C.A.C. Sequeira, Sodium borohydride as a fuel for the future, Renew. Sustain. Energy Rev. 15 (2011) 3980–4001, http://dx.doi.org/10.1016/j.rser.2011.07.018.
[2] R.K. Ahluwalia, T.Q. Hua, J.-K. Peng, Fuel cycle efficiencies of different automotive on-board hydrogen storage options, Int. J. Hydrogen Energy 32 (2007) 3592–3602, http://dx.doi.org/10.1016/j.ijhydene.2007.03.021.
[3] U.B. Demirci, P. Miele, Sodium tetrahydroborate as energy/hydrogen carrier, its history, Comptes Rendus Chim. 12 (2009) 943–950, http://dx.doi.org/10.1016/j.crci.2008.08.002.
[4] S.S. Muir, X. Yao, Progress in sodium borohydride as a hydrogen storage material: development of hydrolysis catalysts and reaction systems, Int. J. Hydrogen Energy 36 (2011) 5983–5997, http://dx.doi.org/10.1016/j.ijhydene.2011.02.032.
[5] N. Patel, R. Fernandes, A. Miotello, Promoting effect of transition metal-doped Co–B alloy catalysts for hydrogen production by hydrolysis of alkaline $NaBH_4$ solution, J. Catal. 271 (2010) 315–324, http://dx.doi.org/10.1016/j.jcat.2010.02.014.
[6] S.C. Amendola, S.L. Sharp-goldman, M.S. Janjua, N.C. Spencer, M.T. Kelly, P.J. Petillo, et al., A safe, portable, hydrogen gas generator using aqueous borohydride solution and Ru catalyst, Int. J. Hydrogen Energy 25 (2000) 969–975.
[7] H.I. Schlesinger, H.C. Brown, H.R. Hoekstra, L.R. Rapp, Reactions of diborane with alkali metal hydrides and their addition compounds. New syntheses of borohydrides. Sodium and potassium borohydrides1, J. Am. Chem. Soc. 205 (1953) 199.
[8] H.I. Schlesinger, H.C. Brown, A.E. Finholt, The preparation of sodium borohydride by the high temperature reaction of sodium hydride with borate esters, J. Am. Chem. Soc. 1504 (1953) 205–209.
[9] H.I. Schlesinger, H.C. Brown, A.E. Finholt, J.R. Gilbreath, H.R. Hoekstra, E.K. Hyde, Sodium borohydride, its hydrolysis and its use as a reducing agent and in the generation of hydrogen, J. Am. Chem. Soc. 199 (1963).
[10] U.B. Demirci, O. Akdim, J. Andrieux, J. Hannauer, R. Chamoun, P. Miele, Sodium borohydride hydrolysis as hydrogen generator: issues, state of the art and applicability upstream from a fuel cell, Fuel Cells 10 (2010) 335–350, http://dx.doi.org/10.1002/fuce.200800171.
[11] U.B. Demirci, P. Miele, Sodium borohydride versus ammonia borane, in hydrogen storage and direct fuel cell applications, Energy Environ. Sci. 2 (2009) 627, http://dx.doi.org/10.1039/b900595a.
[12] U.B. Demirci, P. Miele, Cobalt in $NaBH_4$ hydrolysis, Phys. Chem. Chem. Phys. 12 (2010) 14651–14665, http://dx.doi.org/10.1039/c0cp00295j.
[13] R. Fernandes, N. Patel, a. Miotello, R. Jaiswal, D.C. Kothari, Stability, durability, and reusability studies on transition metal-doped Co–B alloy catalysts for hydrogen production, Int. J. Hydrogen Energy 36 (2011) 13379–13391, http://dx.doi.org/10.1016/j.ijhydene.2011.08.021.
[14] A. Lu, Y. Chen, J. Jin, G.-H. Yue, D.-L. Peng, CoO nanocrystals as a highly active catalyst for the generation of hydrogen from hydrolysis of sodium borohydride, J. Power Sources 220 (2012) 391–398, http://dx.doi.org/10.1016/j.jpowsour.2012.08.010.
[15] O. Akdim, U.B. Demirci, P. Miele, Deactivation and reactivation of cobalt in hydrolysis of sodium borohydride, Int. J. Hydrogen Energy 36 (2011) 13669–13675, http://dx.doi.org/10.1016/j.ijhydene.2011.07.125.
[16] H. Dai, Y. Liang, P. Wang, X. Yao, T. Rufford, M. Lu, et al., High-performance cobalt–tungsten–boron catalyst supported on Ni foam for hydrogen generation from alkaline sodium borohydride solution, Int. J. Hydrogen Energy 33 (2008) 4405–4412, http://dx.doi.org/10.1016/j.ijhydene.2008.05.080.
[17] H.-B. Dai, G.-L. Ma, X.-D. Kang, P. Wang, Hydrogen generation from coupling reactions of sodium borohydride and aluminum powder with aqueous solution of cobalt chloride, Catal. Today 170 (2011) 50–55, http://dx.doi.org/10.1016/j.cattod.2010.10.094.
[18] V.I. Simagina, O.V. Komova, a. M. Ozerova, O.V. Netskina, G.V. Odegova, D.G. Kellerman, et al., Cobalt oxide catalyst for hydrolysis of sodium borohydride and ammonia borane, Appl. Catal. A Gen. 394 (2011) 86–92, http://dx.doi.org/10.1016/j.apcata.2010.12.028.
[19] L. Damjanović, M. Majchrzak, S. Bennici, A. Auroux, Determination of the heat evolved during sodium borohydride hydrolysis catalyzed by Co_3O_4, Int. J. Hydrogen Energy 36 (2011) 1991–1997, http://dx.doi.org/10.1016/j.ijhydene.2010.11.041.
[20] Y. Liang, P. Wang, H.-B. Dai, Hydrogen bubbles dynamic template preparation of a porous Fe–Co–B/Ni foam catalyst for hydrogen generation from hydrolysis of alkaline sodium borohydride solution, J. Alloys Compd. 491 (2010) 359–365, http://dx.doi.org/10.1016/j.jallcom.2009.10.183.
[21] H.-B. Bin Dai, Y. Liang, P. Wang, Effect of trapped hydrogen on the induction period of cobalt–tungsten–boron/nickel foam catalyst in catalytic hydrolysis reaction of sodium borohydride, Catal. Today 170 (2011) 27–32, http://dx.doi.org/10.1016/j.cattod.2010.09.007.
[22] B. Weng, Z. Wu, Z. Li, H. Yang, H. Leng, Enhanced hydrogen generation by hydrolysis of $LiBH_4$ doped with multiwalled carbon nanotubes for micro proton exchange membrane fuel cell application, J. Power Sources 196 (2011) 5095–5101, http://dx.doi.org/10.1016/j.jpowsour.2011.01.080.
[23] Y. Huang, Y. Wang, R. Zhao, P. Shen, Z. Wei, Accurately measuring the hydrogen generation rate for hydrolysis of sodium borohydride on multiwalled carbon nanotubes/Co–B catalysts, Int. J. Hydrogen Energy 33 (2008) 7110–7115, http://dx.doi.org/10.1016/j.ijhydene.2008.09.046.
[24] D. Xu, H. Wang, Q. Guo, S. Ji, Catalytic behavior of carbon supported Ni–B, Co–B and Co–Ni–B in hydrogen generation by hydrolysis of KBH_4, Fuel Process. Technol. 92 (2011) 1606–1610, http://dx.doi.org/10.1016/j.fuproc.2011.04.006.
[25] L. Yang, N. Cao, C. Du, H. Dai, K. Hu, W. Luo, et al., Graphene supported cobalt(0) nanoparticles for hydrolysis of ammonia borane, Mater. Lett. 115 (2014) 113–116, http://dx.doi.org/10.1016/j.matlet.2013.10.039.
[26] Z.P. Li, B.H. Liu, F.F. Liu, D. Xu, A composite of borohydride and super absorbent polymer for hydrogen generation, J. Power Sources 196 (2011) 3863–3867, http://dx.doi.org/10.1016/j.jpowsour.2010.11.003.
[27] O. Akdim, R. Chamoun, U.B. Demirci, Y. Zaatar, A. Khoury, P. Miele, Anchored cobalt film as stable supported catalyst for hydrolysis of sodium borohydride for chemical hydrogen storage, Int. J. Hydrogen Energy 36 (2011) 14527–14533, http://dx.doi.org/10.1016/j.ijhydene.2011.07.051.
[28] L. Ai, X. Gao, J. Jiang, In situ synthesis of cobalt stabilized on macroscopic biopolymer hydrogel as economical and recyclable catalyst for hydrogen generation from sodium borohydride hydrolysis, J. Power Sources 257 (2014)

213–220, http://dx.doi.org/10.1016/j.jpowsour.2014.01.119.
[29] F. Seven, N. Sahiner, Poly(acrylamide-co-vinyl sulfonic acid) p(AAm-co-VSA) hydrogel templates for Co and Ni metal nanoparticle preparation and their use in hydrogen production, Int. J. Hydrogen Energy 38 (2012) 777–784, http://dx.doi.org/10.1016/j.ijhydene.2012.10.072.
[30] A. Chinnappan, H.-C. Kang, H. Kim, Preparation of PVDF nanofiber composites for hydrogen generation from sodium borohydride, Energy 36 (2011) 755–759, http://dx.doi.org/10.1016/j.energy.2010.12.048.
[31] N. Sahiner, S. Sagbas, The use of poly(vinyl phosphonic acid) microgels for the preparation of inherently magnetic Co metal catalyst particles in hydrogen production, J. Power Sources 246 (2014) 55–62, http://dx.doi.org/10.1016/j.jpowsour.2013.07.043.
[32] S. Butun, N. Sahiner, A versatile hydrogel template for metal nano particle preparation and their use in catalysis, Polym. Guildf. 52 (2011) 4834–4840, http://dx.doi.org/10.1016/j.polymer.2011.08.021.
[33] N. Sahiner, O. Ozay, N. Aktas, E. Inger, J. He, The on demand generation of hydrogen from Co-Ni bimetallic nano catalyst prepared by dual use of hydrogel: as template and as reactor, Int. J. Hydrogen Energy 36 (2011) 15250–15258, http://dx.doi.org/10.1016/j.ijhydene.2011.08.082.
[34] F. Seven, N. Sahiner, Enhanced catalytic performance in hydrogen generation from $NaBH_4$ hydrolysis by super porous cryogel supported Co and Ni catalysts, J. Power Sources 272 (2014) 128–136, http://dx.doi.org/10.1016/j.jpowsour.2014.08.047.
[35] R. Chamoun, B. Demirci, D. Cornu, Y. Zaatar, R. Khoury, a Khoury, et al., From soil to lab: utilization of clays as catalyst supports in hydrogen generation from sodium borohydride fuel, Fuel 90 (2011) 1919–1926, http://dx.doi.org/10.1016/j.fuel.2010.11.037.
[36] J.W. Jaworski, S. Cho, Y. Kim, J.H. Jung, H.S. Jeon, B.K. Min, et al., Hydroxyapatite supported cobalt catalysts for hydrogen generation, J. Colloid Interface Sci. 394 (2013) 401–408, http://dx.doi.org/10.1016/j.jcis.2012.11.036.
[37] Q. Li, H. Kim, Hydrogen production from $NaBH_4$ hydrolysis via Co-ZIF-9 catalyst, Fuel Process. Technol. 100 (2012) 43–48, http://dx.doi.org/10.1016/j.fuproc.2012.03.007.
[38] M. Rakap, S. Özkar, Intrazeolite cobalt(0) nanoclusters as low-cost and reusable catalyst for hydrogen generation from the hydrolysis of sodium borohydride, Appl. Catal. B Environ. 91 (2009) 21–29, http://dx.doi.org/10.1016/j.apcatb.2009.05.014.
[39] S.C. Amendola, S.L. Sharp-Goldman, M.S. Janjua, M.T. Kelly, P.J. Petillo, M. Binder, An ultrasafe hydrogen generator: aqueous, alkaline borohydride solutions and Ru catalyst, J. Power Sources 85 (2000) 186–189, http://dx.doi.org/10.1016/S0378-7753(99)00301-8.
[40] S.J. Kim, J. Lee, K.Y. Kong, C. Ryul Jung, I.-G. Min, S.-Y. Lee, et al., Hydrogen generation system using sodium borohydride for operation of a 400W-scale polymer electrolyte fuel cell stack, J. Power Sources 170 (2007) 412–418, http://dx.doi.org/10.1016/j.jpowsour.2007.03.083.
[41] Y. Kojima, K. Suzuki, K. Fukumoto, Y. Kawai, M. Kimbara, H. Nakanishi, et al., Development of 10 kW-scale hydrogen generator using chemical hydride, J. Power Sources 125 (2004) 22–26, http://dx.doi.org/10.1016/S0378-7753(03)00827-9.
[42] G.M. Arzac, a. Fernández, a. Justo, B. Sarmiento, M. a. Jiménez, M.M. Jiménez, Optimized hydrogen generation in a semicontinuous sodium borohydride hydrolysis reactor for a 60W-scale fuel cell stack, J. Power Sources 196 (2011) 4388–4395, http://dx.doi.org/10.1016/j.jpowsour.2010.10.073.
[43] J. Lee, T. Kim, Micro PEM fuel cell system with $NaBH_4$ hydrogen generator, Sens. Actuators A Phys. 177 (2012) 54–59.
[44] S.C. Amendola, M. Binder, S.L. Sharp-Goldman, M.T. Kelly, P.J. Petillo, System for hydrogen generation, US 6534033 B1, 2003.
[45] S.C. Amendola, P.J. Petillo, S.C. Petillo, Method and apparatus for precessing discharged fuel solution from a hydrogen generator, WO 2004/007354 A1, 2004.
[46] J. V. Ortega, Y. Wu, S.C. Amendola, M.T. Kelly, Processes for synthesizing alkali metal borohydride compounds, WO 051957 A1, 2003.
[47] R.M. Mohring, P.J. Petillo, S.C. Amendola, K.A. Fennimore, Differential pressure-driven borohydride based generator, WO 006150 A1, 2003.
[48] S.C. Amendola, P.J. Petillo, S.C. Petillo, R.M. Mohring, Portable hydrogen generator, WO 2003/004145 A1, 2003.
[49] S.C. Amendola, P.J. Petillo, S.C. Petillo, R.M. Mohring, Portable hydrogen generator, US 6932847 B2, 2005.
[50] R.W. Grimes, A.N. Fitch, Thermal decomposition of cobalt(II) acetate tetrahydrate studied with time-resolved neutron diffraction and thermogravimetric analysis, J. Mater. Chem. 1 (1991) 461–468.
[51] F.M. Hochella Jr., G.E. Brown Jr., F.K. Ross, G.V. Gibbs, High-temperature crystal chemistry of hydrous Mg- and Fe-cordierites, Am. Mineral. 64 (1979) 337. http://www.minsocam.org/ammin/AM64/AM64_337.pdf.
[52] XRPD data were extracted from PDF-2 containing ICDD (International Centre for Diffraction Data) experimental powder data collection: http://www.icdd.com.
[53] B.D. Hall, D. Zanchet, D. Ugarte, Estimating nanoparticle size from diffraction measurements, J. Appl. Crystallogr. 33 (2000) 1335–1341, http://dx.doi.org/10.1107/S0021889800010888.
[54] S. Menchetti, C. Sabelli, A new borate polyanion in the structure of $N_8[B_{12}O_{20}(OH)_4]$, Acta Crystallogr. Sect. B Struct. Crystallogr. Cryst. Chem. 35 (1979) 2488–2493, http://dx.doi.org/10.1107/S0567740879009742.
[55] S. Choi, L.D.S. Lapitan, Y. Cheng, T. Watanabe, Synthesis of cobalt boride nanoparticles using RF thermal plasma, Adv. Powder Technol. 25 (2014) 365–371, http://dx.doi.org/10.1016/j.apt.2013.06.002.
[56] U.B. Demirci, P. Miele, Cobalt-based catalysts for the hydrolysis of $NaBH_4$ and NH_3BH_3, Phys. Chem. Chem. Phys. 16 (2014) 6872–6885, http://dx.doi.org/10.1039/c4cp00250d.
[57] U.B. Demirci, O. Akdim, J. Hannauer, R. Chamoun, P. Miele, Cobalt, a reactive metal in releasing hydrogen from sodium borohydride by hydrolysis: a short review and a research perspective, Sci. China Chem. 53 (2010) 1870–1879, http://dx.doi.org/10.1007/s11426-010-4081-1.
[58] A. Garron, D. Swierczynski, S. Bennici, A. Auroux, New insights into the mechanism of H_2 generation through $NaBH_4$ hydrolysis on Co-based nanocatalysts studied by differential reaction calorimetry, Int. J. Hydrogen Energy 34 (2009) 1185–1199, http://dx.doi.org/10.1016/j.ijhydene.2008.11.027.